Eur J Nucl Med Mol Imaging (2012) 39:1128–1136
DOI 10.1007/s00259-012-2129-5

ORIGINAL ARTICLE

# Concomitant radio- and fluorescence-guided sentinel lymph node biopsy in squamous cell carcinoma of the oral cavity using ICG-$^{99m}$Tc-nanocolloid

**Nynke S. van den Berg · Oscar R. Brouwer · W. Martin C. Klop · Bariş Karakullukcu · Charlotte L. Zuur · I. Bing Tan · Alfons J. M. Balm · Michiel W. M. van den Brekel · Renato A. Valdés Olmos · Fijs W. B. van Leeuwen**

Received: 8 February 2012 / Accepted: 20 March 2012 / Published online: 18 April 2012


**Abstract**
*Purpose* For oral cavity malignancies, sentinel lymph node (SLN) mapping is performed by injecting a radiocolloid around the primary tumour followed by lymphoscintigraphy. Surgically, SLNs can then be localized using a handheld gamma ray detection probe. The aim of this study was to evaluate the added value of intraoperative fluorescence imaging to the conventional radioguided procedure. For this we used indocyanine green (ICG)-$^{99m}$Tc-nanocolloid, a hybrid tracer that is both radioactive and fluorescent.
*Methods* Fourteen patients with oral cavity squamous cell carcinoma were peritumourally injected with ICG-$^{99m}$Tc-nanocolloid. SLNs were preoperatively identified with lymphoscintigraphy followed by single photon emission computed tomography (SPECT)/CT for anatomical localization. During surgery, SLNs were detected with a handheld gamma ray detection probe and a handheld near-infrared fluorescence camera. Pre-incision and post-excision imaging with a portable gamma camera was performed to confirm complete removal of all SLNs.
*Results* SLNs were preoperatively identified using the radioactive signature of ICG-$^{99m}$Tc-nanocolloid. Intraoperatively, 43 SLNs could be localized and excised with combined radio- and fluorescence guidance. Additionally, in four patients, an SLN located close to the primary injection site (in three patients this SLN was located in level I) could only be intraoperatively localized using fluorescence imaging. Pathological analysis of the SLNs revealed a metastasis in one patient.
*Conclusion* Combined preoperative SLN identification and intraoperative radio- and fluorescence guidance during SLN biopsies for oral cavity cancer proved feasible using ICG-$^{99m}$Tc-nanocolloid. The addition of fluorescence imaging was shown to be of particular value when SLNs were located in close proximity to the primary tumour.

**Keywords** Near-infrared fluorescence · Image-guided surgery · Sentinel lymph node biopsy · Multimodal imaging · Oral cavity squamous cell carcinoma

Nynke S. van den Berg and Oscar R. Brouwer contributed equally to the study.

**Electronic supplementary material** The online version of this article (doi:10.1007/s00259-012-2129-5) contains supplementary material, which is available to authorized users.

N. S. van den Berg · O. R. Brouwer · R. A. Valdés Olmos (✉) · F. W. B. van Leeuwen
Department of Nuclear Medicine, The Netherlands Cancer Institute–Antoni van Leeuwenhoek Hospital, Plesmanlaan 121, 1066 CX Amsterdam, The Netherlands
e-mail: r.valdes@nki.nl

W. M. C. Klop · B. Karakullukcu · C. L. Zuur · I. B. Tan · A. J. M. Balm · M. W. M. van den Brekel
Department of Head & Neck Surgery and Oncology, The Netherlands Cancer Institute–Antoni van Leeuwenhoek Hospital, Plesmanlaan 121, 1066 CX Amsterdam, The Netherlands

N. S. van den Berg · F. W. B. van Leeuwen
Department of Radiology, Interventional Molecular Imaging Section, Leiden University Medical Center, Albinusdreef 2 (C2-S zone), P.O. Box 9600, 2300 RC Leiden, The Netherlands

## Introduction

The incidence of lymph node metastases in patients with squamous cell carcinoma of the oral cavity is 20–30% [1, 2]. By using sentinel lymph node (SLN) biopsy to select patients with occult metastases, an unnecessary elective neck dissection (END) may be avoided in 70–80% of patients [1, 3]. SLN biopsy has several advantages over END: (1) reduced morbidity [4]; (2) improved identification of so-called skip metastases and aberrant lymphatic drainage patterns [5–7]; and (3) improved pathological specimen analysis for the detection of (micro-)metastases [8, 9]. For SLN biopsy, overall sensitivity rates of 91% after 5-year follow-up have been reported [10]. However, for floor of mouth (FOM) tumours, the sensitivity and the negative predictive values were much lower compared to other sites, 80 vs 97% and 88 vs 98%, respectively [10]. A prospective multi-institutional trial reported false-negative rates of 25 and 10% for FOM and tongue tumours, respectively, whereas this was said to be 0% for other types of oral cavity cancers [11]. In oral cavity malignancies, SLNs are often located in close proximity to the primary tumour site, which can render SLN biopsy difficult.

Conventional SLN mapping is performed by injecting a radiocolloid ($^{99m}$Tc-nanocolloid or $^{99m}$Tc-sulphur colloid) in or around the primary tumour followed by sequential lymphoscintigraphy to identify the lymph nodes on a direct drainage pathway from the primary tumour (the SLNs) [12]. To provide an overview of the SLNs with regard to their anatomical location, single photon emission computed tomography combined with computed tomography (SPECT/CT) was introduced. Additionally, with SPECT/CT more SLNs can be visualized compared to conventional lymphoscintigraphy [13]. Intraoperatively, SLN localization is commonly guided by the acoustic signal coming from a handheld gamma ray detection probe. However, since for oral cavity cancers SLNs are often located in close proximity to the primary tumour site, the high radioactive background signal coming from the injection site may hamper intraoperative radioguidance towards these SLNs [6, 14]. Recently, the intraoperative use of a portable gamma camera was shown to improve the localization of SLNs near the injection site [15].

Vital blue dyes are generally applied to enable intraoperative visual detection of the SLNs, but have shown to be of limited value in oral cavity tumours as SLNs in the head and neck area are less frequently stained blue compared to other primary tumour sites [16–18]. Moreover, the use of blue dye may blur the visibility of intraoral tumour margins [1, 19].

To enable visual detection of SLNs without affecting the surgical field, the near-infrared (NIR) fluorescence tracer indocyanine green (ICG) was introduced for SLN mapping in various tumour types such as breast, colon and gastric cancers [20, 21]. Recently, Bredell evaluated the use of ICG for SLN mapping in oropharyngeal cancer [22]. ICG is not visible by the naked eye and does, therefore, not interfere with the visual identification of tumour margins [23]. However, similar to vital blue dyes, ICG rapidly migrates through the lymphatic system leading to a limited diagnostic window and staining of higher echelon nodes [24]. To address these migratory limitations of optical dyes, the self-assembled hybrid radiocolloid ICG-$^{99m}$Tc-nanocolloid was clinically introduced for selective SLN biopsy [25, 26]. In this complex, ICG adopts the lymphatic migration properties of the radiocolloid, resulting in a significantly longer retention time in the SLNs as compared to ICG alone. With this hybrid tracer being both radioactive and fluorescent, preoperative surgical planning can be combined with intraoperative radioguidance towards the SLNs. The fluorescent properties of the hybrid tracer extend the radioguided procedure by providing real-time optical localization using an NIR fluorescence camera. For head and neck melanoma it was shown that with this approach fluorescence-based SLN identification was superior over the use of blue dye [26]. The aim of the current study was to explore the utility of the hybrid tracer during SLN biopsy for squamous cell carcinoma of the oral cavity.

## Materials and methods

### Patients

Between May 2011 and January 2012, 14 patients with squamous cell carcinoma of the oral cavity were included in this study after obtaining written informed consent. Patients were scheduled for surgical removal of the primary tumour followed by SLN biopsy. All patients were staged with T1/2 tumours and were clinically node negative as assessed by ultrasound and fine-needle aspiration cytology (USFNAC). Further patient characteristics are listed in Table 1. The study protocol was approved by the Institution's Medical Ethics Committee.

### Tracer preparation

$^{99m}$Tc-Nanocolloid was prepared by adding 1,400 MBq pertechnetate in 2 ml saline to a vial of nanocolloid (GE Healthcare, Eindhoven, The Netherlands). The mixture was then incubated for 30 min at room temperature after which the excess of reactive elements was removed. Before adding ICG, a quality check was performed in which the colour, clarity and pH were determined (colourless, clear and pH 6–7, respectively).

ICG was prepared by adding 5 ml sterile water to a vial containing 25 mg ICG (vial concentration 5 mg/ml; Pulsion Medical Systems, Munich, Germany). Then, 50 μl of ICG solution was added to the $^{99m}$Tc-nanocolloid to form ICG-$^{99m}$Tc-nanocolloid.

**Table 1** Patient characteristics

| | | | | | Preoperative imaging | | Intraoperative findings | | | | Pathology |
|---|---|---|---|---|---|---|---|---|---|---|---|
| | Age (years) | Sex | Tumour location | Time injection–surgery (h) | Total no. of defined SLNs | SLN location | Radioguidance | Fluorescence guidance | Total no. of excised SLNs | Location additional excised SLNs | Tumour-positive nodes |
| 1 | 61 | M | FOM midline | 4 | 2 | R level III; L level III | 3 | 3 | 3 | R level III | 0 |
| 2 | 51 | M | Tongue R | 5 | 2 | R level I, level III | 2 | 2 | 2 | | 0 |
| 3 | 58 | F | FOM L | 19 | 2 | L level I, level III | 3 | 3 | 3 | L level III | 0 |
| 4 | 62 | F | Tongue R | 5 | 3 | R level I, level II; L level III | 3 | 3 | 3 | | 0 |
| 5 | 59 | F | Tongue R | 4 | 2 | R level II, level III | 1 | 2 | 2 | | 1 |
| 6 | 84 | F | Buccal mucosa R | 19 | 1 | R level II | 1 | 1 | 1 | | 0 |
| 7 | 82 | M | Tongue L | 19 | 3 | L level II, 2×level III | –[a] | –[a] | 0 | | - |
| 8 | 74 | M | Lower lip L | 5 | 5 | R level III; L 3×level I, level III | 7 | 7 | 7 | L 2×level I | 0 |
| 9 | 61 | F | FOM R | 4 | 4 | L 2×level III, level I; R level III | 3 | 4 | 4 | | 0 |
| 10 | 65 | M | Tongue R | 4 | 4 | R level I, level II; L level II, level III | 4[b] | 4[b] | 4[b] | R level II | 0 |
| 11 | 75 | M | Tongue L | 4 | 1 | L level II | 3 | 3 | 3 | L 2×level II | 0 |
| 12 | 60 | M | FOM midline | 4 | 4 | L level I, level III; R level III, level IV | 5 | 6 | 6 | R 2×level III | 0 |
| 13 | 71 | M | Tongue R | 3 | 3 | R level II; L level III, level V | 3 | 3 | 3 | | 0 |
| 14 | 54 | F | FOM midline | 4 | 5 | L level I, level III; R level I, level II, level III | 5 | 6 | 6 | L level I | 0 |
| Total | | | | | 41 | | 43 | 47 | 47 | | 1 |

*SLN* sentinel lymph node, *LN* lymph node, *M* male, *F* female, *FOM* floor of mouth, *R* right, *L* left

[a] In this patient, the SLN procedure was ceased

[b] In this patient, the L level II SLN was not excised

All procedures were performed under good manufacturing practice (GMP-z) and under supervision of the institution's pharmacist.

### Tracer administration and preoperative imaging

A median of 77 MBq (range 67–94 MBq) ICG-$^{99m}$Tc-nanocolloid was injected in three or four deposits around the primary tumour (total volume 0.4 ml; Fig. 1). To visualize the lymphatic duct(s) with the subsequent SLN (s), anterior and lateral dynamic images were obtained during the first 10 min after injection using a dual-head gamma camera (Symbia T, Siemens, Erlangen, Germany). Static planar gamma camera images were acquired 15 min and 2 h post-injection (Fig. 2a). The latter was immediately followed by SPECT/CT (Symbia T, Siemens, Erlangen, Germany; Fig. 2b). SPECT and CT images were obtained on the basis of 2-mm slices. After tissue attenuation correction for the SPECT, fused SPECT/CT images were generated. SPECT, CT and fused SPECT/CT were simultaneously evaluated using orthogonal multiplanar reconstruction. In addition, 3-D display using volume rendering was performed in order to improve anatomical neck level recognition (Fig. 2c).

SLNs were defined as the lymph nodes on a direct lymphatic drainage pathway from the primary tumour [12]. Early draining lymph nodes in a basin were considered to be the SLNs in case of multiple visualized lymph nodes without visible afferent vessels.

### Surgical procedure

SLN biopsy started 3–19 h after ICG-$^{99m}$Tc-nanocolloid administration. In the operating room, a portable gamma camera (Sentinella equipped with Sentinella suite software version 7.5; Oncovision, Valencia, Spain) was used to acquire a pre-incision overview image (Fig. 3b, pre-incision) and to determine the location for the incision(s) [15]. Initial SLN exploration was guided by a handheld gamma ray detection probe (Neoprobe, Johnson & Johnson Medical, Hamburg, Germany; Fig. 3d). Fluorescence imaging with a dedicated handheld NIR fluorescence camera (PhotoDynamic Eye, Hamamatsu Photonics, Hamamatsu, Japan; Fig. 3e) was used to optically detect the SLNs. After excision of the SLN(s), the portable gamma camera was used to search for remaining radioactive hot spots in the SLN excision area (Fig. 3b, post-excision) as was previously described by Vermeeren et al. [15]. Second echelon nodes (defined by preoperative lymphoscintigraphy and SPECT/CT) were left in situ.

### Pathology

Harvested SLNs were fixed in formalin, bisected, embedded in paraffin, cut at a minimum of six levels at 50- to 150-μM intervals and histologically evaluated for the presence of (micro-)metastases (haematoxylin and eosin (H&E) and anti-cytokeratin (CAM 5.2; Becton Dickinson, San Jose, CA, USA) staining).

## Results

### Preoperative findings

Distribution of tumour locations in the 14 included patients was as follows: FOM ($n$=5), tongue ($n$=7), lower lip ($n$=1) and buccal mucosa ($n$=1). Further patient characteristics and the pre- and intraoperative findings of all 14 patients are outlined in Table 1. A schematic overview of primary tumour and intraoperative SLN location is provided in Fig. 4a and b, respectively.

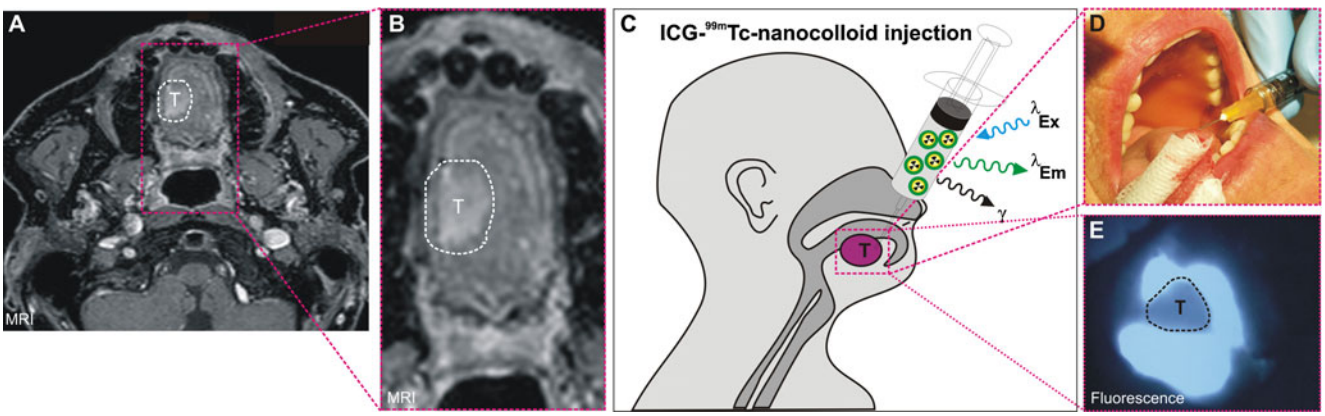


**Fig. 1** Hybrid ICG-$^{99m}$Tc-nanocolloid injection surrounding the primary tumour site. **a** Axial diagnostic MRI image showing a tumour on the tongue (*T*). **b** Zoom in on the tongue tumour. **c–d** ICG-$^{99m}$Tc-nanocolloid is peritumourally injected in three to four deposits. **e** Intraoperative, NIR fluorescence-based visualization of the injection sites (*T* tumour)

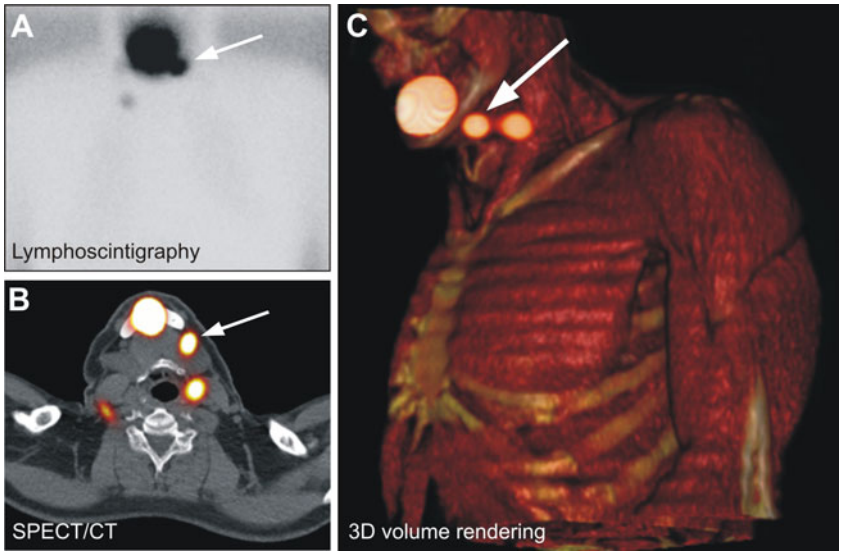


**Fig. 2** Preoperative SLN identification. **a** A late planar anterior lymphoscintigram 2 h post-injection showing two SLNs on the right side and one SLN on the left side (*arrow*). **b** Axial SPECT/CT slice showing two level II SLNs (bilateral) and a level I SLN close to the injection site (*arrow*). **c** The 3-D volume rendered SPECT/CT showing two SLNs on the left side, in level I (*arrow*) and level II (these SLNs were not visible as separate hot spots on the planar lymphoscintigram)

Lymphatic drainage was visualized in all patients. Bilateral lymphatic drainage was found in eight patients. In only 3 of these patients (patients 1, 12 and 14) the tumour had crossed the midline. Using conventional lymphoscintigraphy, a total of 37 SLNs were visualized. Four additional SLNs were only visible on the SPECT/CT images in 3 patients (patients 8, 9 and 12) resulting in a total of 41 preoperatively defined SLNs (median of 3 SLNs per patient; range 1–5) dispersed over 34 basins (median of 2 basins per patient; range 1–5 basins per patient) (Table 1). In all 14 patients, the fused SPECT/CT images provided an accurate anatomical reference point for surgical planning of the SLN biopsy procedure, including the SLNs that were found to be located close to the primary injection site (an example is given in Fig. 2).

## Intraoperative findings

The SLN biopsy procedure started 3–19 h post ICG-$^{99m}$Tc-nanocolloid injection and could be completed in all but 2 patients (patients 7 and 10; Table 1). A total of 47 SLNs (median of 3 SLNs per patient; range 0–7) was intraoperatively detected and excised; 43 SLNs could be intraoperatively localized with the combined radio- and fluorescence guidance approach (Fig. 4b). In 4 patients (patients 5, 9, 12 and 14), a total of 4 SLNs were found to be located close to the injection site (level I or II; Table 1 and Fig. 4b). In these patients, SLN identification with the handheld gamma ray detection probe was hampered due to the high background signal coming from the injection site (Fig. 3). Although the portable gamma camera was able to distinguish these SLNs from the injection site after masking the injection site using the "blackout zone" function (Fig. 3b), fluorescence imaging proved to be the most accurate technology for the identification of these SLNs during surgery. To optimize fluorescence-based SLN identification, lights were dimmed in the operating room. The SLNs could be pointed out or taken hold of with a surgical forceps (Fig. 3e). Subsequently, the light was turned back on and the SLN could be excised.

In 4 patients (patients 3, 8, 10 and 12), a total of 7 additional SLNs were identified with the handheld gamma ray detection probe. These SLNs were not previously identified as separate hot spots on the preoperative images (most probably these SLNs were part of a cluster of SLNs). These nodes also proved to be fluorescent and were subsequently harvested. Post-excision control with the portable gamma camera revealed residual radioactivity in the excision area in 3 patients (patients 1, 11 and 14). This resulted in the removal of three additional SLNs, again guided by a combination of handheld gamma probe tracing and fluorescence imaging.

In two patients, the SLN biopsy was not completed to prevent possible vital structure damage. In patient 7 an SLN was located medially of the mandible and very close to the main trunk of the facial nerve (see Supporting Information Fig. S1). Despite successful detection with the handheld gamma ray detection probe and the portable gamma camera, visualization of this SLN with the NIR fluorescence camera was not possible. In patient 10, an SLN was located near branches of the marginal mandibular nerve. This SLN could be detected with the portable gamma camera, but its exact location could not be identified with the handheld gamma ray detection probe. Initial exploration with the NIR fluorescence camera also did not reveal the location of the SLN. To reduce the invasiveness of the procedure and to prevent the possible risk of paresis of the lower lip, it was decided not to proceed with the excision. In both cases, the lack of a fluorescent signal suggested that the SLN left in situ was located >0.5 cm deeper from the surface imaged; the

penetration depth of ICG is limited to 0.5–1.0 cm (Fig. 3). Both patients will be closely monitored following the "watch and wait" protocol.

### Pathological findings

Although the SLNs were clearly defined in vivo by fluorescence imaging, it was impossible to solely dissect the single SLN separately in 5 patients (patients 1, 5, 8, 10 and 13). Subsequently, in these patients some additional tissue was also excised. This resulted in the identification of 13 additional lymph nodes in these tissue specimens. All of these lymph nodes were evaluated as SLNs.

Histopathological examination revealed SLNs with largest diameters varying from 2 to 25 mm with a median of 6 mm. In one patient (patient 5) a level III lymph node metastasis of 3 mm was found. This patient received a subsequent therapeutic neck dissection during which 34 additional tumour-negative lymph nodes from level I–V were removed.

## Discussion

The present study shows that a single injection of ICG-$^{99m}$Tc-nanocolloid enables preoperative SLN mapping and intraoperative radio- and fluorescence-guided identification of the SLNs draining from primary oral cavity cancers. SPECT/CT and the portable gamma camera allowed for accurate surgical planning, even when SLNs were found in close proximity to the injection site. Intraoperatively, surgeons experienced the optical detection of the SLNs provided by the fluorescent label of the hybrid tracer as valuable, especially in cases where localization with the handheld gamma ray detection probe was impeded by high radioactive background signals. In FOM

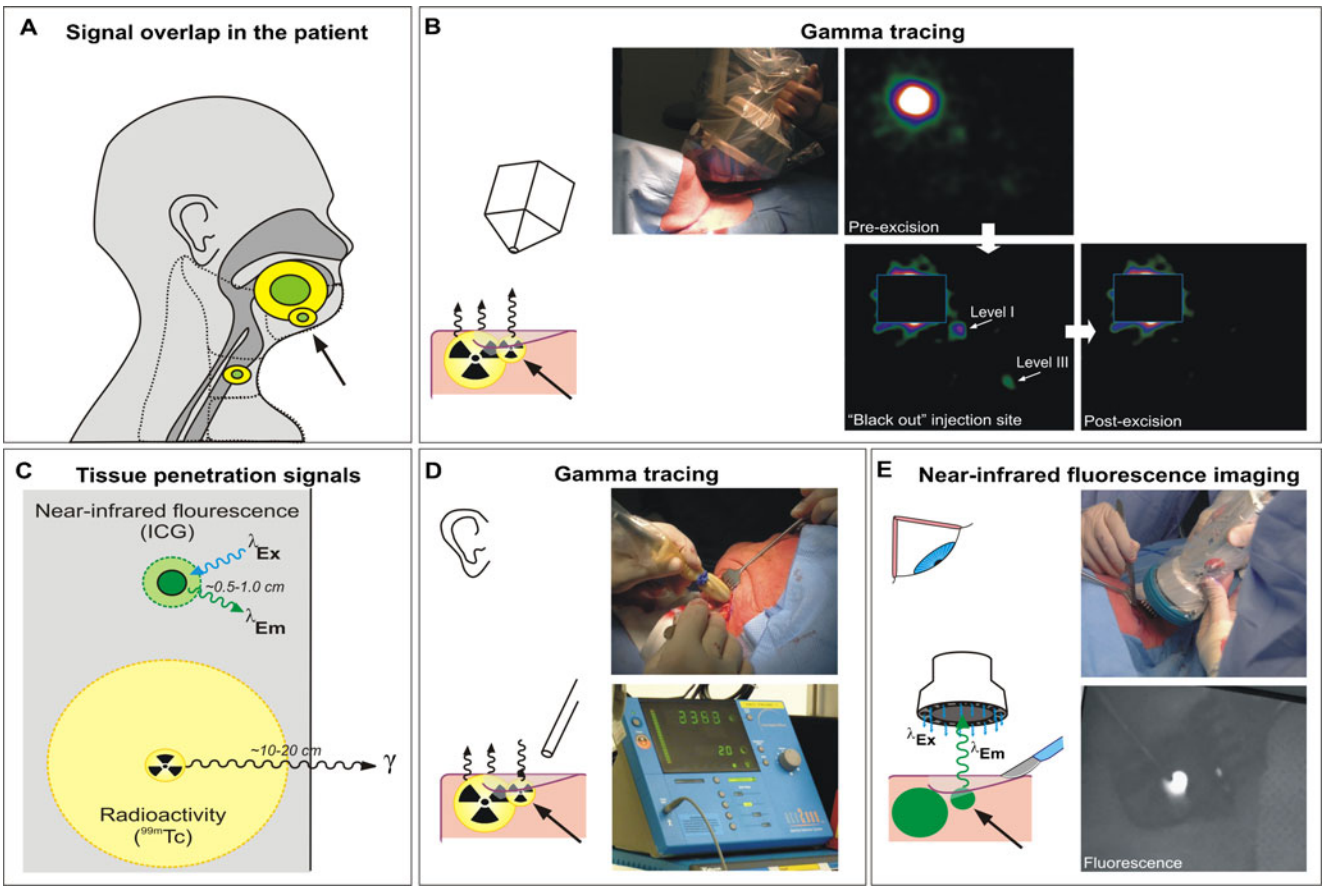


**Fig. 3** Intraoperative SLN identification. **a** Schematic overview depicting how detection of an SLN residing close to the primary tumour/injection site (*arrow*) can be difficult with radioguidance alone because of the high background signal coming from the injection site. **b** Intraoperative gamma imaging with a portable gamma camera is performed before and after excision of the SLN(s) to localize and to confirm complete removal of all predetermined SLNs, respectively. The "blackout zone" feature of the portable gamma camera enables masking of the primary injection site, increasing the signal intensities of the weaker radioactive hot spots. **c** The fluorescence signal penetration depth of the NIR dye ICG is limited to approximately 0.5–1.0 cm, whereas the penetration depth of the radioactive signal is much greater depending on the imaging modality used. **d** Intraoperatively, SLNs are acoustically traced with a handheld gamma ray detection probe. **e** NIR fluorescence imaging allows for visual identification and excision of the SLN(s)

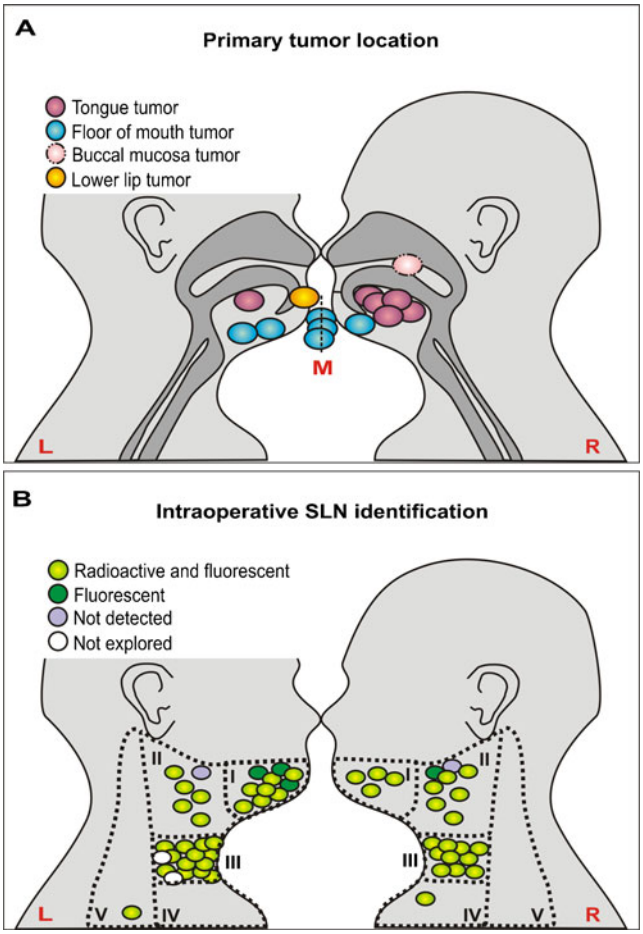


**Fig. 4** Schematic overview of primary tumour location and the intraoperative SLN identification results. **a** Primary tumour location. *L* left, *R* right, *M* midline. **b** Intraoperative SLN identification method. The nodes that could be best identified with NIR fluorescence imaging during surgery (green dots in the figure) were also radioactive

tumours, SLN biopsy is discouraged due to its low sensitivity [10] which we reason may partially be a result of the difficulty to intraoperatively localize such SLNs in the vicinity of the injection site. The addition of fluorescence imaging to the conventional radioguided procedure may be of particular benefit in this patient group. In this study, a total of four SLNs was found in level I in the five patients with FOM tumours. Three (75%) of these could only be accurately detected with fluorescence imaging.

Contralateral lymph node involvement ranges from 0.9 to 34.7% [27]. Bilateral lymphatic drainage was observed on the lymphoscintigrams in 54% ($n$=8) of patients, even though the primary tumour had crossed the midline in only three of these patients. Hence, by performing an upfront unilateral END, such (potentially tumour-positive) contralateral draining nodes might be missed.

With the rise of minimally invasive surgery, SLN biopsy becomes more favourable over END procedures. Lymph nodes are generally small (3–4 mm) and are frequently found in close proximity to each other [18]. These conditions create high demands on the limited spatial resolution of the handheld gamma ray detection probe. In the current study, the high spatial resolution (down to the micrometre level) provided by fluorescence imaging enabled the detection and removal of individual SLNs as small as 2 mm.

The use of a non-covalent self-assembly approach to generate imaging agents is appealing as it allows for the formation of hybrid agents by combining "simple" and often commercially available, clinically approved building blocks [28]. The hybrid tracer ICG-$^{99m}$Tc-nanocolloid was built from $^{99m}$Tc-nanocolloid particles (used for conventional SLN mapping in Europe) and the NIR fluorescent dye ICG. GMP-z preparation of ICG-$^{99m}$Tc-nanocolloid only adds one additional step to the conventional radiocolloid preparation process, namely the addition of 0.25 mg ICG to a solution of fully prepared $^{99m}$Tc-nanocolloid. The pH of the $^{99m}$Tc-nanocolloid solution is 6–7, and therefore the preparation protocol does not negatively influence the optical properties of ICG [29]. With this hybrid approach SLNs could be accurately visualized using approximately 100 times lower quantities of ICG compared to the study of Bredell [22]. Although one may reason that non-covalent particles may disintegrate in vivo, a large degree of signal overlap was found in the lymphatic system in both preclinical models [24, 30, 31] and in patients [25, 26]. In none of our clinical studies performed thus far did we find nodes that solely contained a fluorescent or a radioactive signal [25, 26].

The use of ICG alone for SLN mapping of oropharyngeal cancer was set to be optimal 5 min post ICG injection [22], while in the current study SLNs were still fluorescent at 19 h after ICG-$^{99m}$Tc-nanocolloid injection. Clearly the retention of the hybrid tracer in the SLNs yields a superior diagnostic window. It therefore does not require additional (intraoperative) injections which helps to optimize the logistics in daily practice.

The limited penetration depth of fluorescence imaging compared to modalities based on radioactivity may even be useful, since it can help the surgeon to estimate the depth at which an SLN can be localized in order to decide if further exploration is needed (as described for patients 7 and 10).

The NIR fluorescence signal coming from ICG is invisible to the naked eye and can only be visualized with a dedicated NIR fluorescence camera system. As such ICG does not interfere with primary tumour margin visibility [23] like blue dyes do. This study demonstrates how optical guidance provided by the hybrid tracer's fluorescent label offers an excellent alternative over visual blue dyes and facilitates accurate SLN localization, even when an SLN resides in close proximity to the primary tumour.

Supplementing the conventional radioguided SLN biopsy procedure with fluorescence only moderately increases the costs of the procedure as the NIR fluorescence imaging system used in this study is in the same price range as a

handheld gamma ray detection probe. The costs of ICG are also not higher than that of the original tracer $^{99m}$Tc-nanocolloid and one vial of ICG can be used for multiple tracer preparations.

## Conclusion

In conclusion, the hybrid tracer ICG-$^{99m}$Tc-nanocolloid allows for both preoperative lymphatic mapping and intraoperative SLN detection up to 19 h post-injection. The added guidance provided by fluorescence imaging proved especially valuable for the detection of SLNs located close to the primary tumour site.

**Acknowledgements** This work was partially supported in part by the Dutch Cancer Society translational research award (Grant No. PGF 2009–4344; FvL) and NWO-STW-VIDI (Grant No. STW BGT11271; NvdB and FvL).

We gratefully thank the entire surgical staff, hospital pharmacy and technical support of the Nuclear Medicine Department for their contribution and Professor T.J.M. Reurs for kindly providing the fluorescence camera system.

## References

1. Broglie MA, Stoeckli SJ. Relevance of sentinel node procedures in head and neck squamous cell carcinoma. Q J Nucl Med Mol Imaging 2011;55(5):509–20.
2. Coughlin A, Resto VA. Oral cavity squamous cell carcinoma and the clinically n0 neck: the past, present, and future of sentinel lymph node biopsy. Curr Oncol Rep 2010;12(2):129–35.
3. Stoeckli SJ, Alkureishi LW, Ross GL. Sentinel node biopsy for early oral and oropharyngeal squamous cell carcinoma. Eur Arch Otorhinolaryngol 2009;266(6):787–93.
4. Murer K, Huber GF, Haile SR, Stoeckli SJ. Comparison of morbidity between sentinel node biopsy and elective neck dissection for treatment of the n0 neck in patients with oral squamous cell carcinoma. Head Neck 2011;33(9):1260–4.
5. Byers RM, Weber RS, Andrews T, McGill D, Kare R, Wolf P. Frequency and therapeutic implications of "skip metastases" in the neck from squamous carcinoma of the oral tongue. Head Neck 1997;19(1):14–9.
6. Civantos FJ, Moffat FL, Goodwin WJ. Lymphatic mapping and sentinel lymphadenectomy for 106 head and neck lesions: contrasts between oral cavity and cutaneous malignancy. Laryngoscope 2006;112(3 Pt 2 Suppl 109):1–15.
7. Stoeckli SJ. Sentinel node biopsy for oral and oropharyngeal squamous cell carcinoma of the head and neck. Laryngoscope 2007;117(9):1539–51.
8. Civantos Jr F, Zitsch R, Bared A, Amin A. Sentinel node biopsy for squamous cell carcinoma of the head and neck. J Surg Oncol 2008;97(8):683–90.
9. Stoeckli SJ, Pfaltz M, Ross GL, Steinert HC, MacDonald DG, Wittekind C, et al. The second international conference on sentinel node biopsy in mucosal head and neck cancer. Ann Surg Oncol 2005;12(11):919–24.
10. Alkureishi LW, Ross GL, Shoaib T, Soutar DS, Robertson AG, Thompson R, et al. Sentinel node biopsy in head and neck squamous cell cancer: 5-year follow-up of a European multicenter trial. Ann Surg Oncol 2010;17(9):2459–64.
11. Civantos FJ, Zitsch RP, Schuller DE, Agrawal A, Smith RB, Nason R, et al. Sentinel lymph node biopsy accurately stages the regional lymph nodes for T1-T2 oral squamous cell carcinomas: results of a prospective multi-institutional trial. J Clin Oncol 2010;28(8):1395–400.
12. Nieweg OE, Tanis PJ, Kroon BB. The definition of a sentinel node. Ann Surg Oncol 2001;8(6):538–41.
13. Vermeeren L, Valdés Olmos RA, Klop WM, van der Ploeg IM, Nieweg OE, Balm AJ, et al. SPECT/CT for sentinel lymph node mapping in head and neck melanoma. Head Neck 2011;33(1):1–6.
14. de Bree R, Leemans CR. Recent advances in surgery for head and neck cancer. Curr Opin Oncol 2010;22(3):186–93.
15. Vermeeren L, Valdés Olmos RA, Klop WM, Balm AJ, van den Brekel MW. A portable gamma-camera for intraoperative detection of sentinel nodes in the head and neck region. J Nucl Med 2010;51(5):700–3.
16. Chao C, Wong SL, Edwards MJ, Ross MI, Reintgen DS, Noyes RD, et al. Sentinel lymph node biopsy for head and neck melanomas. Ann Surg Oncol 2003;10(1):21–6.
17. Eicher SA, Clayman GL, Myers JN, Gillenwater AM. A prospective study of intraoperative lymphatic mapping for head and neck cutaneous melanoma. Arch Otolaryngol Head Neck Surg 2002;128(3):241–6.
18. Tanis PJ, Nieweg OE, van den Brekel MW, Balm AJ. Dilemma of clinically node-negative head and neck melanoma: outcome of "watch and wait" policy, elective lymph node dissection, and sentinel node biopsy–a systematic review. Head Neck 2008;30(3):380–9.
19. Kuriakose MA, Trivedi NP. Sentinel node biopsy in head and neck squamous cell carcinoma. Curr Opin Otolaryngol Head Neck Surg 2009;17(2):100–10.
20. Polom K, Murawa D, Rho YS, Nowaczyk P, Hünerbein M, Murawa P. Current trends and emerging future of indocyanine green usage in surgery and oncology: a literature review. Cancer 2011;117(21):4812–22.
21. Schaafsma BE, Mieog JS, Hutteman M, van der Vorst JR, Kuppen PJ, Löwik CW, et al. The clinical use of indocyanine green as a near-infrared fluorescent contrast agent for image-guided oncologic surgery. J Surg Oncol 2011;104(3):323–32.
22. Bredell MG. Sentinel lymph node mapping by indocyanin green fluorescence imaging in oropharyngeal cancer - preliminary experience. Head Neck Oncol 2010;2:31.
23. Vahrmeijer AL, Frangioni JV. Seeing the invisible during surgery. Br J Surg 2011;98(6):749–50.
24. van Leeuwen AC, Buckle T, Bendle G, Vermeeren L, Valdés Olmos R, van de Poel HG, et al. Tracer-cocktail injections for combined pre- and intraoperative multimodal imaging of lymph nodes in a spontaneous mouse prostate tumor model. J Biomed Opt 2011;16(1):016004.
25. van der Poel HG, Buckle T, Brouwer OR, Valdés Olmos RA, van Leeuwen FW. Intraoperative laparoscopic fluorescence guidance to the sentinel lymph node in prostate cancer patients: clinical proof of concept of an integrated functional imaging approach using a multimodal tracer. Eur Urol 2011;60(4):826–33.
26. Brouwer OR, Klop WM, Buckle T, Vermeeren L, van den Brekel MW, Balm AJ, et al. Feasibility of sentinel node biopsy in head and neck melanoma using a hybrid radioactive and fluorescent tracer. Ann Surg Oncol 2011. doi:10.1245/s10434-011-2180-7.
27. González-Garcia R, Naval-Gías L, Rodríguez-Campo FJ, Sastre-Pérez J, Muñoz-Guerra MF, Gil-Díez Usandizaga JL. Contralateral lymph neck node metastasis of squamous cell carcinoma of the oral cavity: a retrospective analytic study in 315 patients. J Oral Maxillofac Surg 2008;66(7):1390–8.

28. Buckle T, Chin PT, van Leeuwen FW. (Non-targeted) radioactive/fluorescent nanoparticles and their potential in combined pre- and intraoperative imaging during sentinel lymph node resection. Nanotechnology 2010;21(48):482001.
29. Björnsson OG, Murphy R, Chadwick VS, Björnsson S. Physiochemical studies on indocyanine green: molar lineic absorbance, pH tolerance, activation energy and rate of decay in various solvents. J Clin Chem Clin Biochem 1983;21(7):453–8.
30. Buckle T, van Leeuwen AC, Chin PT, Janssen H, Muller SH, Jonkers J, et al. A self-assembled multimodal complex for combined pre- and intraoperative imaging of the sentinel lymph node. Nanotechnology 2010;21(35):355101.
31. Bunschoten A, Buckle T, Kuil J, Luker GD, Luker KE, Nieweg OE, et al. Targeted non-covalent self-assembled nanoparticles based on human serum albumin. Biomaterials 2012;33(3):867–75.